Pair approximation for the dimer-dimer-monomer surface reaction model

1998 J. Phys. A: Math. Gen. 31 7751

(http://iopscience.iop.org/0305-4470/31/38/010)

J. Phys. A: Math. Gen. **31** (1998) 7751–7760. Printed in the UK PII: S0305-4470(98)89411-0

Pair approximation for the dimer–dimer–monomer surface reaction model

Zhonghuai Hou, Lingfa Yang and Houwen Xin†

Department of Chemical Physics, University of Science and Technology of China, Hefei, Anhui, 230026, People's Republic of China

Received 21 November 1997, in final form 31 March 1998

Abstract. In this work, the authors construct a pair-approximation (PA) mean-field theory (MFT) for the dimer–dimer–monomer surface reaction model proposed by E V Albano. We find that PA-MFT can yield predictions which are qualitatively and quantitatively in good agreement with the Monte Carlo simulation results. We conclude that PA-MFT may be suitable to describe these kinds of lattice-gas models and it is likely to make predictions using PA-MFT ahead of Monte Carlo simulation.

1. Introduction

Recently, the subject of reaction kinetics and irreversible phase transitions (IPTs) in surface catalysis has gained growing attention. Since one lacks a general theory to study nonequilibrium phase transition, great efforts have been concentrated on Monte Carlo simulations (MCS) and corresponding theoretical descriptions for particular models. The simplest model is the monomer–monomer (MM) model [4–12], $A + B \rightarrow 0$, for which a single first-order critical point exists at $y_{1A} = \frac{1}{2}$, such that for $y_A < y_{1A}$ ($y_A > y_{1A}$)(here y_A denotes the normalized rate of arrival and subsequent sticking coefficient of A-species, which is proportional to the mole fraction of A-species in the gas phase), the surface is poisoned by B- (A-)species, respectively. Inspired by the carbon monoxide oxidation $CO + \frac{1}{2}O_2 \rightarrow CO_2$ on a catalyst surface, the dimer–monomer (DM) model $A + \frac{1}{2}B_2 \rightarrow AB$ (A and B_2 correspond to CO and O_2, respectively) has been extensively studied by means of various techniques ever since the work of Ziff, Gulari and Barshad (so the DM model is also known as the ZGB model) [13–32]. There exist two IPTs for this model, one of second order at $y_{1A} \simeq 0.391$ and the other of first order at $y_{2A} \simeq 0.525$, between which is a reaction window where sustained reaction occurs. The counterpart of the dimer–dimer (DD) [33–36] model, $\frac{1}{2}B_2 + C_2 \rightarrow BC_2$, in real systems is the catalytic oxidation of hydrogen (B_2 (C_2) corresponds to O_2 (H_2) respectively). A first-order phase transition exists at the stoichiometric value $y_{1c} = \frac{2}{3}$. Based on these models Albano [1–3] studied two multiple-reaction models: one is the dimer–monomer–monomer (DMM) model [37–38] which is the combination of the DM model and the MM model, and the other is the dimer–dimer–monomer (DDM) [1–3] model which combines the DM model and the DD model and will be studied in this work. Although neither of these two models represents any specific real reaction system, they are helpful to study the influence of contaminants on the critical

† Author to whom correspondence should be addressed.

0305-4470/98/387751+10$19.50

behaviour of the well known IPTs characteristic of the MM, the DM and the DD models. Furthermore, they also exhibit rich critical behaviours, i.e. they both have a continuous set of both first- and second-order IPTs.

Some theoretical approaches [14, 15, 18, 24, 26–28, 30–34] have also been proposed to study these kinds of IPTs. Among these approaches, mean-field theory (MFT) within pair approximation (PA), proposed by Dickman [15, 18] can qualitatively well reproduce the phase diagrams and even quantitatively yield correct predictions of the first-order IPT values for the ZGB model. In our previous works, we have adopted PA-MFT to some variants of the ZGB model [30], the (extended) DMM model [38] and the DD model [36]. Dumont *et al* has used PA-MFT to study the isotopic exchange surface reaction [32]. It is found that PA-MFT also shows good agreement with MCS for these models. Note that these models are all based on the Langmuir–Hinshelwood (LH) mechanism, i.e. all reactants are adsorbed on the surface. Different species adsorbed on adjacent pairs of sites react instantaneously such that each reaction step concerns two nearest-neighbour (NN) sites; on the other hand, the adsorption of a dimer also needs a pair of adjacent empty sites. Therefore NN correlation plays a very important role in these surface reaction models, and PA-MFT, which takes into account NN correlation, can reasonably describe the steady state behaviours of these models.

In this work, we shall construct a PA-MFT for the DDM model. For comparison, we have also performed MCS. The aim of this work is to study the critical behaviour of the IPTs characteristic of this multiple-reaction model by a theoretical approach and further demonstrate the validity of PA-MFT. One notes that MCS often needs a large amount of computing time due to the use of a large lattice and critical slowing down [1] in the vicinity of IPTs. As an example, the CPU time required to obtain a single point in figure 1(a) is about 2.5 h using a lattice of side $L = 150$. Evaluation of the critical points, such as those shown in figure 3 (broken line), need much more time and typically requires about 20 h of CPU time per single point. However, using PA-MFT, one only needs about 1.5 h to obtain a single point in figure 3 (full line). Thus, it may be more convenient to use PA-MFT to predict some interesting characters of the extended DDM model, such as the influence of diffusion, desorption, finite reaction probability [31] and so on, rather than MCS.

The DDM model is based on the LH mechanism and it is assumed the reaction occurs according to the following steps:

$$A(g) + S \rightarrow A(a) \tag{1a}$$

$$B_2(g) + 2S \rightarrow 2B(a) \tag{1b}$$

$$C_2(g) + 2S \rightarrow 2C(a) \tag{1c}$$

$$A(a) + B(a) \rightarrow AB(g) + S \tag{1d}$$

$$B(a) + C(a) \rightarrow BC(a) + S \tag{1e}$$

$$BC(a) + C(a) \rightarrow BC_2(g) + 2S \tag{1f}$$

where S denotes an empty site, (a) and (g) refer to the adsorbed and gaseous species, respectively. Equations (1a), (1b) and (1d) correspond to the ZGB model and equations (1b), (1c), (1e) and (1f) correspond to the DD model.

In the simulation, the catalyst surface is modelled by a two-dimensional square lattice using periodic boundary conditions. In each simulation step, A, B_2 and C_2 are selected at random with probability y_A, y_B and y_C ($y_A + y_B + y_C = 1$), respectively. Note that a selected dimer needs two adjacent empty sites for adsorption. After a successful adsorption of each species, the neighbourhood is checked for reactions (1d–f). A random decision is made when more than one reaction path is possible, but reactions (1d) and (1f) take

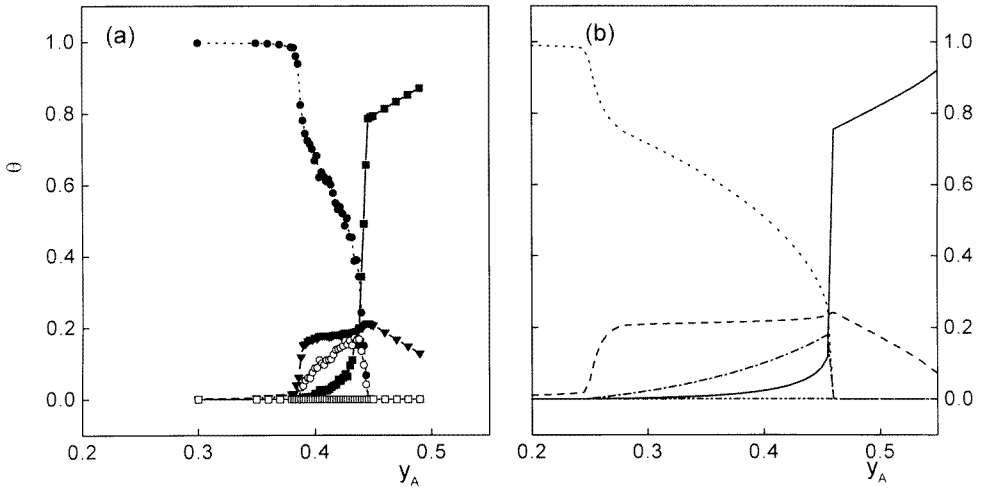

Figure 1. Phase diagrams for $y_C = 0.0005$ obtained from MCS and PA-MFT. ——(full square): θ_A; ·····(full circle): θ_B; – – –(down triangle): θ_{BC}. (*a*) For MCS the two IPTs exist at $y_{1A} = 0.3825$ and $y_{2A} = 0.446$. (*b*) For PA-MFT $y_{1A} = 0.243$ and $y_{2A} = 0.457$.

precedence over reaction (1*e*). After a reaction step, the products $AB(g)$ and $C_2B(g)$ are removed from the surface immediately. For more details of the simulation algorithm, see the descriptions of both the ZGB model [13] and the DD model [33–35].

2. Pair approximation for the DDM model

According to PA-MFT, one should derive the equations of motion for the pair-concentrations x_{ij}. For the DDM model, ij can be of type SS, AS, BS, CS, DS, AA, BB, CC, DD, AC, AD and BD (from now on, we often use D to represent $BC(a)$-species for the sake of convenience). It is useful to distinguish between the processes happening on the surface according to their different rates and different contributions to the pair-change numbers (PCNs) ΔN_{ij}. Furthermore, one has to distinguish both between subprocesses leading to different PCNs and between different configurations which might lead to a given process. In this work, we divide the processes into the following three groups:

(1) A-adsorption and following reaction;
(2) B_2-adsorption and following reaction;
(3) C_2-adsorption and following reaction.

In table 1, we list the subprocesses and their rates. Accordingly the PCNs are presented in table 2. The processes are distinguished between each other according to the following facts: for A-adsorption, one just needs to check its neighbourhood for B to account for reaction (1*d*); for B_2-adsorption, since adsorbed B-species can react either with C or with A and reaction (1*d*) takes precedence over (1*e*), one must first decide if there exist A-species in the neighbourhood of the SS-pair where B_2 adsorbs to account for reaction (1*d*), and if not, check for C-species for reaction (1*e*) and possible further reaction (1*f*). The case of C-adsorption is similar as that of B_2. The diagrams in table 1 give examples of the initial configurations of a given subprocess and the notes can help understanding the expressions of the rates. Note that for subprocess (2*b*), the C-species and the SS-pair can be on the same line (not shown in table 1) or not (shown there) for which the rate is $\frac{1}{3}R^{2b}$

Table 1. The subprocesses and their rates for the DDM model.

Process	Diagram	Notes	Rates (R^k)
(1a)	$S \to A$	No B-neighbours for S	$y_a \cdot s \cdot (1-b_s)^4$
(1b)	$SB \xrightarrow{AB\uparrow} SS$	S has B-neighbours	$y_a \cdot s \cdot [1-(1-b_s)^4]$
(2a)	$SS \to BB$	$none + none$(No A; No C)	$y_b \cdot x_{ss} \cdot (1-v)^6$
(2b)	$\begin{matrix} S & S & \xrightarrow{D(a)} & D & B \\ C & & & S & \end{matrix}$	$1C + none$	$y_b \cdot x_{ss} \cdot 6c_s(1-v)^5$
(2c)	$\begin{matrix} S & S & \xrightarrow{2D(a)} & D & D \\ C & C & & S & S \end{matrix}$	$1C + 1C$	$y_b \cdot x_{ss} \cdot 9c_s^2(1-v)^4$
(2d)	$\begin{matrix} C & S & S & \xrightarrow{CD\uparrow} & S & S & B \\ & C & & & S & & \end{matrix}$	$2C + none$	$y_b \cdot x_{ss} \cdot [6c_s^2(1-v)^4 + 2c_s^3(1-v)^3]$
(2e)	$\begin{matrix} C & S & S & \xrightarrow{CD\uparrow+D(a)} & S & S & D \\ & C & C & & & S & S \end{matrix}$	$2C + 1C$	$y_b \cdot x_{ss} \cdot [18c_s^3(1-v)^3 + 6c_s^4(1-v)^2]$
(2f)	$\begin{matrix} C & S & S & C & \xrightarrow{2CD\uparrow} & S & S & S & S \\ & C & C & & & & S & S & \end{matrix}$	$2C + 2C$	$y_b \cdot x_{ss} \cdot [18c_s^4(1-v)^2 + 6c_s^5(1-v) + c_s^6]$
(2g)	$\begin{matrix} S & S & \xrightarrow{AB\uparrow} & S & B \\ A & & & S & \end{matrix}$	$A(s) + none$	$y_b \cdot x_{ss} \cdot 2(1-v)^3 \cdot [1-(1-a_s)^3]$
(2h)	$\begin{matrix} S & S & \xrightarrow{AB\uparrow+D(a)} & S & D \\ A & C & & S & S \end{matrix}$	$A(s) + 1C$	$y_b \cdot x_{ss} \cdot 6c_s(1-v)^2 \cdot [1-(1-a_s)^3]$
(2i)	$\begin{matrix} S & S & C & \xrightarrow{AB\uparrow+CD\uparrow} & S & S & S \\ A & C & & & S & S & \end{matrix}$	$A(s) + 2C$	$y_b \cdot x_{ss} \cdot [6c_s^2(1-v) + c_s^3] \cdot [1-(1-a_s)^3]$
(2j)	$\begin{matrix} S & S & \xrightarrow{2AB\uparrow} & S & S \\ A & A & & S & S \end{matrix}$	$A(s) + A(s)$	$y_b \cdot x_{ss} \cdot [1-(1-a_s)^3]^2$
(3a)	$SS \longrightarrow CC$	$none + none$(No B; No D)	$y_c \cdot x_{ss} \cdot (1-u)^6$
(3b)	$\begin{matrix} S & S & \xrightarrow{D(a)} & S & C \\ B & & & D & \end{matrix}$	$B(s) + none$	$y_c \cdot x_{ss} \cdot 2[(1-d_s)^3 - (1-u)^3] \cdot (1-u)^3$
(3c)	$\begin{matrix} S & S & \xrightarrow{2D(a)} & S & S \\ B & B & & D & D \end{matrix}$	$B(s) + B(s)$	$y_c \cdot x_{ss} \cdot [(1-d_s)^3 - (1-u)^3]^2$
(3d)	$\begin{matrix} S & S & \xrightarrow{CD\uparrow} & S & C \\ D & & & S & \end{matrix}$	$D(s) + none$	$y_c \cdot x_{ss} \cdot 2[1-(1-d_s)^3] \cdot (1-u)^3$
(3e)	$\begin{matrix} S & S & \xrightarrow{CD\uparrow} & S & S \\ D & B & & S & D \end{matrix}$	$D(s) + B(s)$	$y_c \cdot x_{ss} \cdot 2[1-(1-d_s)^3] \cdot [(1-d_s)^3 - (1-u)^3]$
(3f)	$\begin{matrix} S & S & \xrightarrow{2CD\uparrow} & S & S \\ D & D & & S & S \end{matrix}$	$D(s) + D(s)$	$y_c \cdot x_{ss} \cdot [1-(1-d_s)^3]^2$
where	$i_j = \frac{(1+\delta_{ij})x_{ij}}{2x_j}$, here $\delta_{ij} = \begin{cases} 0 & (i \neq j) \\ 1 & (i = j) \end{cases}$;	$u = b_s + d_s$; $v = a_s + c_s$;	$x_i = \frac{1}{2}\sum_j (1+\delta_{ij})x_{ij}$

Table 2. Pair-change-numbers (PCN) for DDM model.

Process	ΔN_{ss}	ΔN_{as}	ΔN_{bs}	ΔN_{cs}	ΔN_{ds}
$(1a)$	$-4\beta_{bss}$	$4(\beta_{bss}-\beta_{bas})$	0	$-4\beta_{bcs}$	$-4\beta_{bds}$
$(1b)$	$1+3s_b$	0	$-1+3b_b-3s_b$	0	$3d_b$
$(2a)$	$-1-6\beta_{vss}$	0	$6(\beta_{vss}-\beta_{vbs})$	0	$-6\beta_{vds}$
$(2b)$	$-1+\frac{7}{3}(s_c-\beta_{vss})$	$\frac{7}{3}(a_c-a_s)$	$\frac{2}{3}+\frac{7}{3}\beta_{vss}-\frac{13}{3}\beta_{vbs}$	$-\frac{5}{3}+\frac{7}{3}(c_c-s_c)$	$1-\frac{13}{3}\beta_{vds}$
$(2c)$	$-1+\frac{2}{9}cc+\frac{43}{9}s_c-\frac{29}{9}\beta_{vss}$	$\frac{43}{9}a_c-\frac{29}{9}a_s$	$-\frac{29}{9}\beta_{vbs}$	$-\frac{25}{9}+\frac{43}{9}(c_c-s_c)$	$\frac{25}{9}+\frac{29}{9}(\beta_{vss}-\beta_{vds})$
$(2d)$	$1+\frac{14}{3}s_c-\frac{5}{3}\beta_{vss}$	$\frac{14}{3}a_c$	$\frac{7}{3}+\frac{5}{3}(\beta_{vss}-\beta_{vbs})$	$-\frac{10}{3}+\frac{14}{3}(c_c-s_c)$	$-\frac{5}{3}\beta_{vds}$
$(2e)$	$1+\frac{4}{9}cc+\frac{65}{9}s_c-\frac{10}{9}\beta_{vss}$	$\frac{65}{9}a_c-\frac{10}{9}\beta_{vas}$	$-\frac{10}{9}\beta_{vbs}$	$-\frac{35}{9}+\frac{43}{9}(c_c-s_c)$	$\frac{26}{9}+\frac{10}{9}(\beta_{vss}-\beta_{vds})$
$(2f)$	$4+\frac{8}{9}cc+\frac{92}{9}s_c$	$\frac{92}{9}a_c$	0	$-4+\frac{92}{9}(c_c-s_c)$	0
$(2g)$	$3(s_a-\beta_{vss})$	$-1+3a_a-3s_a$	$1+3(\beta_{vss}-\beta_{vbs})$	$3c_a$	$3(d_a-\beta_{vds})$
$(2h)$	$\frac{2}{9}ac-2\beta_{vss}+\frac{25}{9}(s_a-s_c)$	$-1-2\beta_{vas}+\frac{25}{9}(a_c+a_a-s_a)$	$-2\beta_{vbs}$	$-1+\frac{25}{9}(c_c+c_a-s_c)$	$2+2(\beta_{vss}-\beta_{vds})+\frac{25}{9}d_a$
$(2i)$	$3+\frac{4}{9}ac+\frac{23}{9}s_a+\frac{50}{9}s_c$	$-1+\frac{23}{9}(s_a-s_a)+\frac{50}{9}a_c$	0	$-2+\frac{50}{9}(c_c-s_c)+\frac{23}{9}c_a$	$\frac{23}{9}d_a$
$(2j)$	$2+\frac{2}{9}aa+\frac{50}{9}s_a$	$-2+\frac{50}{9}(a_a-s_a)$	0	$\frac{50}{9}c_a$	$\frac{50}{9}d_a$
$(3a)$	$-1-6\beta_{uss}$	$-6\beta_{uas}$	0	$6(\beta_{uss}-\beta_{ucs})$	0
$(3b)$	$-\frac{5}{3}-\frac{7}{3}\beta_{uss}$	$-\frac{7}{3}\beta_{uas}$	$-\frac{5}{3}-\frac{7}{3}s_b$	$\frac{5}{3}+\frac{7}{3}(\beta_{uss}-c_s)$	$\frac{5}{3}+\frac{7}{3}s_b$
$(3c)$	0	0	$-2-\frac{50}{9}s_b$	0	$2+\frac{50}{9}s_b$
$(3d)$	$\frac{7}{3}(s_d-\beta_{uss})$	$\frac{7}{3}(a_d-\beta_{uas})$	$\frac{7}{3}b_d$	$\frac{5}{3}+\frac{7}{3}(\beta_{uss}-\beta_{ucs})$	$-\frac{5}{3}+\frac{7}{3}(d_d-s_d)$
$(3e)$	$1+\frac{25}{9}s_d$	$\frac{25}{9}a_d$	$-1+\frac{25}{9}(b_d-s_b)$	0	$\frac{2}{9}bd+\frac{25}{9}(d_d-s_d+s_b)$
$(3f)$	$2+\frac{2}{9}dd+\frac{50}{9}s_d$	$\frac{50}{9}a_d$	$\frac{50}{9}b_d$	0	$-2+\frac{50}{9}(d_d-s_d)$

where $\beta_{ijk}=\frac{(1+\delta_{jk})x_{jk}}{2x_s-x_i}$, $(i=a,b)$
$\beta_{mjk}=\frac{(1+\delta_{jk})x_{jk}}{2x_s-m}$, $(m=u,v)$

Table 2. (Continued.)

Process	ΔN_{aa}	ΔN_{bb}	ΔN_{cc}	ΔN_{dd}	ΔN_{ac}	ΔN_{ad}
$(1a)$	$4\beta_{bas}$	0	0	0	$4\beta_{bcs}$	$4\beta_{bds}$
$(1b)$	0	$-3b_b$	0	0	0	0
$(2a)$	0	$1+6\beta_{vbs}$	0	0	0	0
$(2b)$	0	$\frac{7}{3}\beta_{vbs}$	$-\frac{7}{3}c_c$	$2\beta_{vds}$	$-\frac{7}{3}a_c$	$\frac{7}{3}a_s$
$(2c)$	0	0	$-\frac{2}{9}cc-\frac{43}{9}c_c$	$1+\frac{29}{9}\beta_{vds}$	$-\frac{43}{9}a_c$	$\frac{29}{9}a_s$
$(2d)$	0	$\frac{5}{3}\beta_{vbs}$	$-\frac{14}{3}c_c$	0	$-\frac{14}{3}a_c$	0
$(2e)$	0	0	$-\frac{4}{9}cc-\frac{65}{9}c_c$	$\frac{10}{9}\beta_{vds}$	$-\frac{65}{9}a_c$	$\frac{10}{9}\beta_{vas}$
$(2f)$	0	0	$-\frac{8}{9}cc-\frac{92}{9}c_c$	0	$-\frac{92}{9}a_c$	0
$(2g)$	$-3a_a$	$3\beta_{vbs}$	0	0	$-3a_c$	$-3d_a$
$(2h)$	$-\frac{25}{9}a_a$	0	$-\frac{25}{9}c_c$	$2\beta_{vds}$	$-\frac{2}{9}ac-\frac{25}{9}(a_c+c_a)$	$-\frac{25}{9}d_a+2\beta_{vas}$
$(2i)$	$-\frac{23}{9}a_a$	0	$-\frac{50}{9}c_c$	0	$-\frac{4}{9}ac-\frac{23}{9}c_a-\frac{50}{9}a_c$	$-\frac{23}{9}d_a$
$(2j)$	$-\frac{2}{9}aa-\frac{50}{9}a_a$	0	0	0	$-\frac{50}{9}c_a$	$-\frac{50}{9}d_a$
$(3a)$	0	0	$1+6\beta_{ucs}$	0	$6\beta_{uas}$	0
$(3b)$	0	$-\frac{7}{3}b_b$	$\frac{7}{3}c_s$	$\frac{7}{3}d_b$	$\frac{7}{3}\beta_{uas}$	0
$(3c)$	0	$-\frac{2}{9}bb-\frac{50}{9}b_b$	0	$\frac{2}{9}bb+\frac{50}{9}d_b$	0	0
$(3d)$	0	0	$\frac{7}{3}\beta_{ucs}$	$-\frac{7}{3}d_d$	$\frac{7}{3}\beta_{uas}$	$-\frac{7}{3}a_d$
$(3e)$	0	$-\frac{25}{9}b_b$	0	$\frac{25}{9}(d_b-d_d)$	0	$-\frac{25}{9}a_d$
$(3f)$	0	0	0	$-\frac{2}{9}dd-\frac{50}{9}d_d$	0	$-\frac{50}{9}a_d$

and $\frac{2}{3}R^{2b}$, respectively. This factor must also be considered in the calculation of ΔN_{ij}, e.g. for subprocess (2*b*),

$$\Delta N_{ij}^{(2b)} = \tfrac{1}{3}\Delta N_{ij}(S\ S\ C) + \tfrac{2}{3}\Delta N_{ij}\begin{pmatrix} S & S \\ & C \end{pmatrix}$$

as it is shown in table 2. The other subprocesses are treated in a similar way. For more details of the derivation of the PCN, see [15, 18, 30–32].

The equations of motion read

$$\frac{\mathrm{d}x_{ij}}{\mathrm{d}t} = \sum_k \Delta N_{ij}^{(k)} \cdot R^{(k)} \tag{2}$$

where $R^{(k)}$ are presented in table 1. The reaction rates of $AB(g)$ and $C_2B(g)$ are

$$R_{AB} = R^{1b} + R^{2g} + R^{2h} + R^{2i} + 2R^{2j} \tag{3a}$$

$$R_{C_2B} = R^{2d} + R^{2e} + 2R^{2f} + R^{2i} + R^{3d} + R^{3e} + 2R^{3f}. \tag{3b}$$

Performing numerical integration of equation (2), one can readily obtain the phase diagram and IPT values of the DDM model. After the system reaches the steady state, the reaction rates can be calculated by equation (3). Note that the IPT values may depend on the choice of initial condition for equation (2). As reported in previous works [15, 30], for the ZGB model, PA-MFT obtains a second-order IPT at $y_{1A} = 0.2487$ and a 'spinodal' point at $y_{sA} = 0.561$ when the system evolves from an initially empty lattice. When the lattice is initially half-empty and half-saturated by *A*, the first-order IPT is located at $y_{2A} = 0.524$ which is in correct agreement with the MCS result 0.525. The discrepancy of y_{1A} between PA-MFT and MCS is due to the long correlation length near the second-order IPT, while, according to Evans [18, 19], the discrepancy between y_{sA} and y_{2A} results from the 'metastability' of the system in the interval $y_{2A} < y_A < y_{sA}$. Our recent study shows that the occurrence of metastability may be due to fluctuations in MCS [39]. In the present work, we do not study the effect of the initial condition and the IPT values are all obtained from an initially empty lattice.

2.1. $A + \frac{1}{2}B_2 \rightarrow AB$ *in the presence of* C_2

If $y_C = 0$, the DDM model reduces to the ZGB model, which exhibits two IPTs at $y_{1A} \simeq 0.391$(second order) and $y_{2A} \simeq 0.525$(first order), such that for $y_A < y_{1A}$ ($y_A > y_{2A}$) the surface becomes poisoned by *B*- (*A*-)species, respectively. From MCS we find that, however, a very small contaminant of *C*-species, e.g. $y_C = 0.0005$, reduces y_{2A} drastically to $y_{2A} \simeq 0.446$, while the second-order IPT is slightly shifted to $y_{1A} \simeq 0.3825$. Both above y_{2A} and below y_{1A}, the poisoned state differs from the ZGB model. Within the poisoned state, for $y_A < y_{1A}$, *B* are the majority species but traces of *BC* are also adsorbed; and for $y_A > y_{2A}$, one also has *BC*-intermediates with a considerable coverage ($\theta_{BC} \simeq 0.2$ close to y_{2A}). Within the reaction regime, the coverage of *BC* is nearly a constant: $\theta_{BC} \simeq 0.19$. The phase diagram for $y_C = 0.0005$ is shown in figure 1(*a*). The simulation results obtained here are in agreement with that obtained by Albano.

Setting $y_C = 0.0005$ and performing numerical integration of equation (2), one can find two IPTs at $y_{1A}^m = 0.243$ and $y_{sA}^m = 0.457$ (the superscript '*m*' corresponds to MFT value) compared with PA-MFT results for the ZGB model: $y_{1A}^m = 0.2487$ and $y_{sA}^m = 0.561$. Although the sharp reduction of y_{2A} obtained by MCS is rather surprising, one sees that it can be well reproduced by PA-MFT. In addition, the value of y_{1A}^m is only slightly left-shifted, which is also in good agreement with MCS. Another character of MCS is also reproduced.

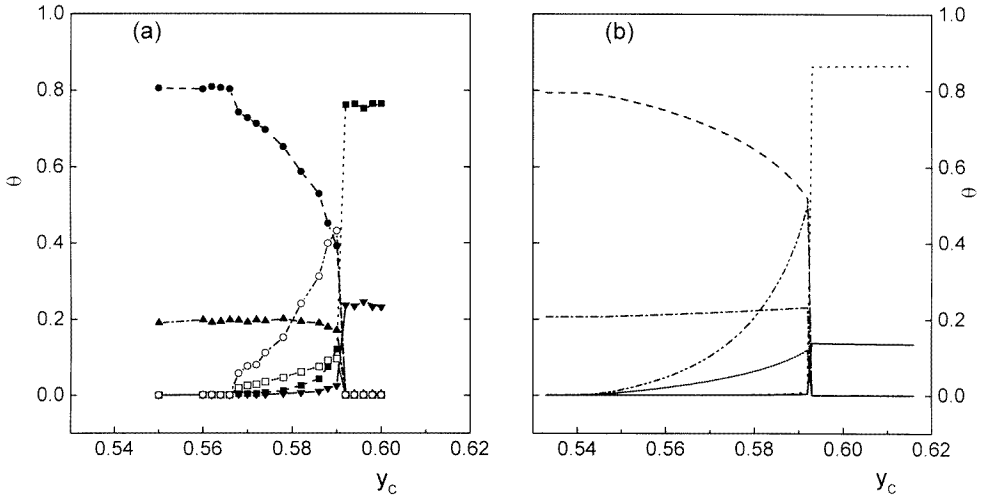

Figure 2. Phase diagram for $y_A = 0.05$ obtained from MCS and PA-MFT. ——(down triangle): θ_A; – – –(full circle): θ_B; · · · · · ·(full square): θ_C; — · —(up triangle): θ_{BC}. (*a*) For MCS $y_{1C} = 0.566$ (second order) and $y_{2C} = 0.592$ (first order). (*b*) For PA-MFT $y_{1C} = 0.544$ and $y_{2C} = 0.593$.

Within the reaction regime, θ_{BC}^m is about 0.21 which is in agreement with the MCS value 0.19. The phase diagram obtained from PA-MFT for $y_C = 0.0005$ is shown in figure 1(*b*). The consistency between figures 1(a) and (b) is rather apparent.

2.2. $\frac{1}{2}B_2 + C_2 \rightarrow BC_2$ *in the presence of A*

If $y_A = 0$ the DDM model reduces to the DD model which has a first-order IPT at the stoichiometric value $y_{1C} = \frac{2}{3}$ such that for $y_C < y_{1C}$ ($y_C > y_{1C}$) the surface becomes poisoned by a binary compound of B- and BC-species (C-species) respectively. One should note that in the poisoned state the total surface coverage is not 1 but $\theta_B + \theta_{BC} \simeq \theta_C \simeq 0.9$. The reason is that the dimer requires adjacent pairs of empty sites for the adsorption.

The presence of monomers A in the gas phase leads to the occurrence of a finite width reaction window. For example, for $y_A = 0.05$ we obtain a second-order IPT at $y_{1C} \simeq 0.566$ and a first-order IPT at $y_{2C} \simeq 0.592$ by MCS. Within the poisoned state, for $y_C < y_{1C}$, the surface is still poisoned by a binary compound of B- and BC-species but now $\theta_B + \theta_{BC} \simeq 1$ because the presence of A-monomers provides a mechanism for the creation of NN empty sites to adsorb dimers, i.e. adsorbed A can react with solitary adsorbed B or C. For $y_C > y_{2C}$, the poisoned state is mainly composed of three species with $\theta_C \gg \theta_A > \theta_{BC}$. The phase diagram obtained from MCS, for $y_A = 0.05$, is shown in figure 2(*a*).

Using PA-MFT, we find $y_{1C}^m = 0.544$ and $y_{2C}^m = 0.593$ for $y_A = 0.05$ which are in reasonable agreement with the MCS results. The phase diagram obtained by PA-MFT is presented in figure 2(*b*). One can see that the main qualitative features in figure 2(*a*) are well reproduced.

2.3. Critical behaviour of the DDM model

Scanning y_A or y_C, the whole range of critical values can be determined and the DDM model shows a crossover from two IPTs charateristic of the DM model ($y_C = 0$) to a first-

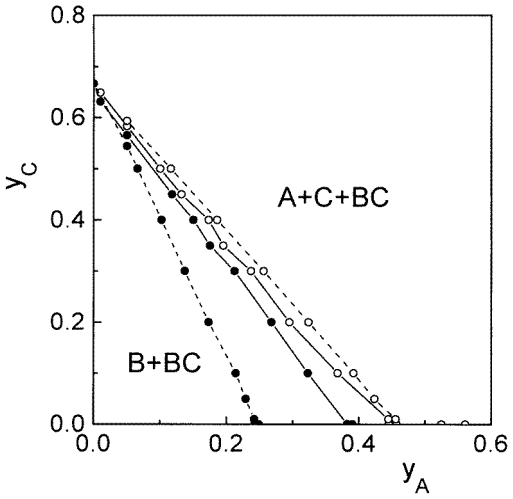

Figure 3. The whole range of critical values obtained from MCS (full lines) and PA-MFT (broken lines). The full circles correspond to first-order IPTs and the open circles to second-order IPTs. The MCS values are mainly drawn from [1].

order IPT of the DD model ($y_A = 0$). In figure 3 we show the whole range of critical values obtained by MCS (full lines) and PA-MFT (broken lines). Note that some of the MCS points are drawn from [1]. The open circles denote first-order IPTs from the reactive regime to a poisoned state with $A + C + BC$, and the full circles represent second-order IPTs from a poisoned state with $B + BC$ to the reactive regime. With increasing y_C in the gas phase, the reactive window characteristic of the DM model becomes increasingly narrow until the two IPTs coincide with each other at the first-order IPT point for the DD model $y_{1C} = \frac{2}{3}$. MCS and PA-MFT are qualitatively in good agreement. On the other hand, one can see that PA-MFT predicts a much wider reaction window than MCS. The drastic left-shift of y_{1A} predicted by PA-MFT results from the large correlation length near the second-order IPT which leads to the breakdown of PA. The overestimation of the first-order IPT values is due to the occurrence of metastability resulting from fluctuations as mentioned above.

3. Conclusion

In this work, we have constructed a PA-MFT method to study the critical behaviour of the DDM reaction model. We find that PA-MFT can well reproduce the phase diagram obtained by MCS and can yield quite good predictions of the influences of the contaminants on the IPTs characteristic of the DM model and the DD model. Our work further demonstrates the validity of PA-MFT on these kinds of lattice-gas models. Since MCS often needs a large amount of computing time due to the use of a large lattice and averaging over many independent runs, we can use this method to study some variants of the DDM model or other interesting multiple-reaction models, e.g. to account for surface diffusion, desorption, finite reaction probability, lateral interaction, and so on. One expects that some interesting predictions can be made ahead of MCS.

Acknowledgment

This work is supported by the National Science Foundation of China. The authors would also like to acknowledge the hospitality of the National Laboratory of Theoretical and Computational Chemistry of China.

References

[1] Albano E V 1994 *Surf. Sci.* **306** 240
[2] Albano E V 1994 *J. Phys. A: Math. Gen.* **27** 3751
[3] Albano E V 1995 *Physica* **214A** 426
[4] Ziff R M and Fichthorn K 1986 *Phys. Rev.* B **34** 2038
[5] Fichthorn K, Gulari E and Ziff R M 1989 *Phys. Rev. Lett.* **63** 1527
[6] Sadiq A and Yaldaram K 1988 *J. Phys. A: Math. Gen.* **21** L207–11
[7] ben Avraham D *et al* 1990 *J. Phys. A: Math. Gen.* **23** 4297
[8] ben Avraham D, Redner S and Meakin P 1990 *J. Phys. A: Math. Gen.* **23** L613
[9] Meakin P and Scalapin D J 1987 *J. Chem. Phys.* **87** 731
[10] Meakin P 1990 *J. Chem. Phys.* **193** 2903
[11] Fichthorn K,Gulari E and Ziff R M 1989 *Chem. Eng. Sci* **44** 1403
[12] Moiny F, Dumont M, Lion J, Dufour P and Dagonnier R 1995 *Surf. Sci.* **325** L392
[13] Ziff R M, Gulari E and Barshad Y 1986 *Phys. Rev. Lett.* **56** 2553
[14] Mai J, von Niessen W and Blumen A 1990 *J. Chem. Phys.* **93** 3685
[15] Dickman R 1986 *Phys. Rev.* A **34** 4246
[16] Brosilow B J and Ziff R M 1992 *Phys. Rev.* A **46** 4534
[17] Ehsasi M, Matioch M, Frank O and Block J H 1989 *J. Chem. Phys.* **91** 4949
[18] Jensen I and Fogedby H C 1990 *Phys. Rev.* A **42** 1969
[19] Evans J W and Miesch M S 1991 *Surf. Sci.* **245** 401
[20] Evans J W and Miesch M S 1991 *Phys. Rev. Lett.* **66** 833
[21] Ziff R M and Brosilow B J 1992 *Phys. Rev.* A **46** 4630
[22] Jensen I, Fogedby H C and Dickman R 1990 *Phys. Rev.* A **41** 3411
[23] Grinstein G, Lai Z W and Browne D A 1989 *Phys. Rev.* A **40** 4820
[24] Evans J W 1993 *J. Chem. Phys.* **98** 2463
[25] Araya P, Porod W, Sant R and Wolf E E 1989 *Surf. Sci.* **208** L80–90
[26] Fischer P and Titulaer P M 1989 *Surf. Sci.* **221** 409–26
[27] Tome T and Dickman R 1992 *Phys. Rev.* E **47** 948
[28] Evans J W 1992 *J. Chem. Phys.* **97** 572
[29] Tammaro M and Evans J W 1995 *Phys. Rev.* E **52** 2310
[30] Hou Z, Yang L and Xin H 1997 *Surf. Sci.* **393** 194
[31] Dumont M, Dufour P, Sente B and Dagonnier R 1990 *J. Catal.* **122** 95
[32] Dumont M, Sente B, Dufour P and Dagonnier R 1992 *J. Chem. Phys.* **96** 4014
[33] Albano E V 1992 *J. Stat. Phys.* **69**
[34] Maltz A and Albano E V 1992 *Surf. Sci.* **277** 414
[35] Albano E V 1992 *J. Phys. A: Math. Gen.* **25** 2557
[36] Hou Z, Yang L and Xin H 1998 *Phys. Rev.* E **58** 234
[37] Albano E V 1996 *J. Phys. A: Math. Gen.* **29** 3317–27
[38] Hou Z, Yang L and Xin H unpublished
[39] Hou Z, Yang L and Xin H 1998 *Surf. Sci.* **399** L332